Available online at www.sciencedirect.com
SCIENCE DIRECT
Catalysis Today 99 (2005) 299–307
CATALYSIS TODAY
www.elsevier.com/locate/cattod

Surface science and electrochemical studies of WC and W_2C PVD films as potential electrocatalysts

Michael B. Zellner[a], Jingguang G. Chen[b,*]

[a]Department of Materials Science and Engineering, Center for Catalytic Science and Technology (CCST), University of Delaware, Newark, DE 19716, USA
[b]Department of Chemical Engineering, Center for Catalytic Science and Technology (CCST), University of Delaware, Newark, DE 19716, USA

Available online 15 December 2004

Abstract

The stability of WC and W_2C in an electrochemical environment has been examined using an electrochemical half-cell in combination with X-ray photoelectron spectroscopy (XPS) to monitor changes in surface composition. The W_2C film is not stable in the electrochemical environment, immediately oxidizing to form surface W_xO_y species. In contrast, the WC film is stable at the anode potential below 0.6 V, demonstrating the potential to be used as an electrocatalyst. In order to determine the feasibility of using WC as an electrocatalyst for direct methanol fuel cells (DMFC), the reaction of methanol on the PVD WC film has been studied using ultrahigh vacuum (UHV) surface techniques, including high-resolution electron energy loss spectroscopy (HREELS) and Auger electron spectroscopy (AES). Methanol dissociates on the WC film to produce the methoxy intermediate (CH_3O), which is stable on the WC surface to 500 K. The reaction of methanol has also been investigated on WC films modified by low coverages of Pt, which shows a promoting effect of Pt for the dissociation of methoxy in the temperature range of 400–500 K. The surface science results suggest a synergistic effect for supporting low coverages of Pt on WC films for the potential application as electrocatalysts.

Keywords: Tungsten carbides; WC; W_2C; PVD film; Methanol; Methoxy; Fuel cells

1. Introduction

This work is a continuation to a series of papers attempting to evaluate the feasibility of using tungsten carbides as fuel cell anode electrocatalysts [1–4]. The anodic chemistry of the direct methanol fuel cell (DMFC) requires the oxidation of methanol and the decomposition of water to produce protons, electrons, and gas-phase CO_2 [5]. Currently, the most effective electrocatalyst for DMFC is the Pt/Ru bimetallic catalyst, which efficiently oxidizes methanol, as well as decomposes water for the oxidation and removal of adsorbed CO species [6–8]. Although the Pt/Ru bimetallic system exhibits desirable electrochemical activities, both Pt and Ru are expensive due to limited supplies. In addition, strong chemisorption of CO on Pt and Ru makes the electrocatalyst susceptible to CO poisoning, blocking the active sites for methanol oxidation. Consequently, discovery of less expensive and more CO tolerant alternatives to the Pt/Ru catalysts would help facilitate the commercialization of DMFC.

A large body of literature exists on the possibility of using transition metal carbides to mimic the catalytic properties of Pt-group metals [9–14]. In particular, there have been many studies on tungsten carbides (WC and W_2C) since Levy and Boudart [15] suggested that WC displayed Pt-like behavior in several catalytic reactions. There have also been several attempts to utilize tungsten carbides as an alternative electrocatalyst due to its stability in acidic solutions at anodic potentials [16,17].

The earlier papers of this series examined reactions of methanol, water, and CO on carbide-modified tungsten (C/W) single crystal surfaces, with and without submonolayer coverages of platinum (Pt/C/W) [1–4]. It was found that 55% and 58% of adsorbed methanol completely decomposes

* Corresponding author. Tel.: +1 302 831 0642; fax: +1 302 831 2085.
E-mail address: jgchen@udel.edu (J.G. Chen).

0920-5861/$ – see front matter © 2004 Elsevier B.V. All rights reserved.
doi:10.1016/j.cattod.2004.10.004

on C/W(1 1 1) and C/W(1 1 0), respectively. The remaining adsorbed methanol dissociates to produce either gas-phase CO or CH_4. Compared to Pt, both C/W(1 1 1) and C/W(1 1 0) also showed significant increases in activity toward the dissociation of water and a reduction in the CO desorption temperatures, both of which would be very desirable for the DMFC application. These surface science results showed the potential for tungsten carbides to be used as anode catalysts in DMFC. However, the reaction pathway that promotes the production of gas-phase CH_4 was undesired due to the loss of four proton/electron pairs per molecule of methanol. Further investigation found that the addition of submonolayer Pt to the C/W(1 1 1) surface eliminated the reaction pathway for gas-phase CH_4, indicating the synergistic effect by supporting low coverages of Pt on C/W(1 1 1).

The current study focuses on bridging the materials gap between model single crystal surfaces and the more realistic, polycrystalline physical vapor deposition (PVD) thin films [18]. Fundamental surface science techniques combined with cyclic voltammetry (CV) measurements have been applied to study the potential application of WC and Pt-modified WC thin films as electrocatalysts in DMFC. This paper begins by characterizing the PVD film composition of W_2C and WC using X-ray diffraction (XRD), followed by testing their stability in an electrochemical environment. Vibrational spectroscopy is then used to study decomposition pathways of methanol on WC and Pt/WC films under ultrahigh vacuum (UHV) conditions. Finally, vibrational spectroscopy is used to examine the adsorption of water and CO on the clean and Pt-modified WC films.

2. Experimental

2.1. Techniques

The UHV chamber used for HREELS measurements has been described in detail previously [12]. The HREEL spectra on the PVD films were acquired with a primary beam energy of 6 eV. Angles of incidence and reflection were 60° with respect to the surface normal in the specular direction. Due to the polycrystalline nature of he PVD films, the intensity and resolution were substantially worse than our previous studies on single crystal surfaces. Count rates in the elastic peak were typically in the range of 1.0×10^4 cps to 1.5×10^4 cps, and the spectral resolution was between 50 and 70 cm^{-1} FWHM (full-width at half maximum). For HREELS experiments the WC film was heated with a linear heating rate of 1.5 K/s.

The UHV chamber used to perform XPS measurements has been described previously [19]. XPS measurements were performed using an ESCALAB MK2 by VG Scientific Ltd. An Al Kα X-ray source of 1486.6 eV was used as the excitation source. All scans were performed with the anode potential of 12 kV and an emission current of 20 mA. The concentric hemispherical analyzer was mounted at 54.7° with respect to the X-ray source and XPS scans were taken under vacuum conditions of approximately 7×10^{-9} Torr for thin films and 5×10^{-10} Torr for single crystals.

CV measurements were performed in an electrochemical half-cell that utilized a three-electrode system consisting of a counter (auxiliary) electrode, a reference electrode, and a working electrode. The counter electrode was a piece of 99.99% pure Pt foil, 0.1 mm thick with a surface area of approximately 6 cm^2. The reference electrode was the saturated calomel electrode ($Hg/Hg_2Cl_2/KCl$), which was measured to be 0.242 V with respect to the normal hydrogen electrode (NHE). The working electrode was the electrocatalyst (WC or W_2C) subject to testing. The tungsten carbides were deposited on a 5 cm × 1 cm carbon paper, coating only the bottom half of the substrate with the electrocatalyst. This working electrode was clamped onto a Pt feedthrough via a Teflon clip inside the cell. The Pt feedthrough was connected to a Princeton Applied Research model 263A potientostat/galvanostat that controlled the potentials of the electrodes. The half-cell used 0.5 M H_2SO_4 as an electrolyte and was sealed in a 1.0 L glass reactor vessel. A Teflon lid and Teflon coated o-rings provided a seal to isolate the reaction chamber from atmosphere and was purged with N_2 to eliminate any air that accumulated during the loading process. A linear potential sweep between the working electrode and the reference electrode, from −0.2 to 1.0 V then back to −0.2 V with respect to the NHE at 10 mV/s, was performed using the potentiostat.

The WC and W_2C thin films were synthesized by magnetron sputtering of a WC target onto glassy carbon substrates for UHV studies and on carbon papers for CV measurements. The W to C ratios were controlled by varying substrate temperature during PVD deposition and by varying temperature and oxygen partial pressure during post-deposition annealing. The result was a single-phase WC or W_2C thin film of approximately 1.0 μm thick. In HREELS measurements, the glassy carbon WC film was wrapped in a tantalum heating jacket that allowed only the tungsten carbide thin film face to be exposed. The jacket was spot welded to two tantalum posts that served as electrical connections for resistive heating, as well as thermal contacts for cooling with liquid nitrogen. A K-type thermocouple was spot welded to the jacket and clamped against the face of the WC film to measure the temperature. With this mounting scheme, the temperature of the WC film could be accurately varied between 200 and 700 K, although lower temperatures were attainable for initial exposures.

Methanol was purchased from Aldrich with >99% purity and was purified by successive freeze-pump-thaw cycles prior to use. The purity was verified in situ by mass spectrometry. In all experiments, the gas exposures were made by backfilling the chamber through leak valves, with the WC and Pt/WC substrate temperatures at 200 K or lower. Doses are reported in Langmuirs (1.0 Langmuir (L) = 1×10^{-6} Torr s) and are uncorrected for ion gauge sensitivity.

2.2. Preparations of clean and Pt-modified WC thin films

The WC thin film surface was cleaned by cycles of Ne^+ bombardment at 450 K (sample current ~5 μA) and flashing to 700 K. These 10-min cycles were generally repeated two times to achieve AES ratio of C/W = 1.0. Auger analysis also showed that oxygen impurities could not be completely removed from the WC thin film after multiple cleaning cycles. AES analysis revealed atomic O/W ratios to be typically at 0.07. Hereafter surfaces with oxygen impurities at or below these levels will be referred to as ''clean'' WC thin films.

The Pt/WC surfaces were prepared via the evaporation of elemental Pt onto the clean WC thin film [20]. The deposition of Pt was achieved by resistively heating a tungsten filament that was wrapped with a thin wire of >99.99% pure Pt. The Pt evaporation source was contained within a tantalum shield, which had an aperture to direct Pt onto the clean WC thin film surface without contaminating the entire UHV chamber. The WC thin film was held at 600 K while deposition occurred. The Pt coverage was estimated from the reduction of the W signal (182 eV) after the deposition of Pt. Although such method is only valid if the growth of Pt occurred in the layer-by-layer faction, the estimate nevertheless provided a qualitative measure of the coverage of Pt on the PVD WC film.

3. Results

3.1. XRD of WC and W_2C thin films

Fig. 1 shows the XRD results for bulk characterization of (a) W_2C and (b) WC thin films on glassy carbon substrates. XRD results of a W_2C thin film, when scanning 2θ from 10 to 80, exhibit the following characteristic features: $2\theta = 34.7$, W_2C 100; $2\theta = 38.2$, W_2C 002; $2\theta = 39.8$, W_2C 101; $2\theta = 52.5$, WC 102; $2\theta = 62.0$, W_2C 110; $2\theta = 70.0$, W_2C 103; and $2\theta = 75.2$, W_2C 112 [21]. Scanning 2θ from 10 to 80, the WC thin film exhibits the following characteristic features: $2\theta = 31.5$, WC 001; $2\theta = 35.8$, WC 100; $2\theta = 48.4$, WC 101; $2\theta = 64.1$–65.7, WC 110; and $2\theta = 73.2$, WC 111 [22]. In addition, broad peaks resulting from the amorphous glassy carbon substrate appear centered at $2\theta = \sim 25$ and $2\theta = \sim 44$. No peaks corresponding to W, W_yC (except $y = 1$ or 2) or WO_x were detected, verifying the phase purity of the W_2C and WC films [21–23].

3.2. Electrochemical stability of W_2C and WC in 0.5 M H_2SO_4

3.2.1. CV measurements of stability

Fig. 2 displays CV curves for (a) a W_2C thin film on carbon paper and (b) a WC thin film on carbon paper submersed in 0.5 M H_2SO_4. The XRD patterns of the WC and W_2C films on carbon papers were identical to those shown in Fig. 1, confirming the phase purity of the WC and W_2C films. For both CV curves, the potential was referenced to the normal hydrogen electrode and anodic current was defined to be positive. Prior to making the CV measurements, nitrogen was purged through the 0.5 M H_2SO_4 electrolyte solution via a gas diffusion stone for 15 min to reduce the effects of residual gas accumulation in the cell during the loading process. The working electrode (WC or W_2C) was then held at 0.05 V for a 45 s conditioning period before being cycled from −0.2 to 1.0 V and back to −0.2 V at a linear rate of 10 mV/s.

The CV curves of W_2C (Fig. 2a) showed a sharp cathodic current at −0.15 V due to recombination of H^+ ions from the sulfuric acid to form H_2 gas. Linearly increasing the potential, the W_2C displayed a region of anodic current beginning at ~−0.1 V, most likely resulting from the oxidation of W_2C into W_xO_y species. Anodic currents persisted until a second, stronger oxidation region of W_2C into W_xO_y species was detected between 0.4 and 0.6 V. Finally a third oxidation region of W_2C at higher potentials was detected as the potential of the W_2C working electrode was linearly increased. As the potential of the working electrode was decreased, decreases in the current occurred due to reduction of the W_xO_y species. At potentials lower than 0 V, recombination of H^+ ions from the sulfuric acid to form H_2 added a strong cathodic current to the existing reduction current of W_xO_y. Fig. 2a compares two consecutive CV scans, which showed a decrease in the oxidation current of the W_2C sample in the second scan. This is because the oxidation reaction of W_2C is not completely reversible during the CV measurements. Decreasing the potential to negative values reduces the W_xO_y species to atomic W and O instead of W_2C. Therefore, a complete CV cycle produces inert surface oxide and diminishes the amount of exposed W_2C. The oxidation current of W_2C continues to decrease after additional CV cycles (not shown).

In contrast, the WC film shows an enhanced stability in 0.5 M H_2SO_4. As shown in Fig. 2b, the CV curve of WC begins with a sharp cathodic current at −0.15 V due to the recombination of H^+ ions in the sulfuric acid to form H_2 gas. Linearly increasing the potential, the WC reaches a stable region from ~0 to ~0.6 V, where no additional increase in current was measured. This behavior was significantly different from that of the W_2C film. At >~0.6 V, the onset of a positive current indicated that the WC film began to oxidize. Further increases in potential beyond ~0.7 V resulted in a dramatic increase in the anodic current due to the oxidation of the WC electrode. Returning from 1.0 to −0.15 V resulted in a slightly negative (or cathodic) current due to reduction of the W_xO_y species formed during the linearly increasing potential period. Below 0 V, cathodic currents from the recombination of H^+ ions added to the cathodic current from the reduction of W_xO_y species, resulting in a sharp decreasing spike. After two consecutive CV scans, a slight decrease in the oxidation current of the

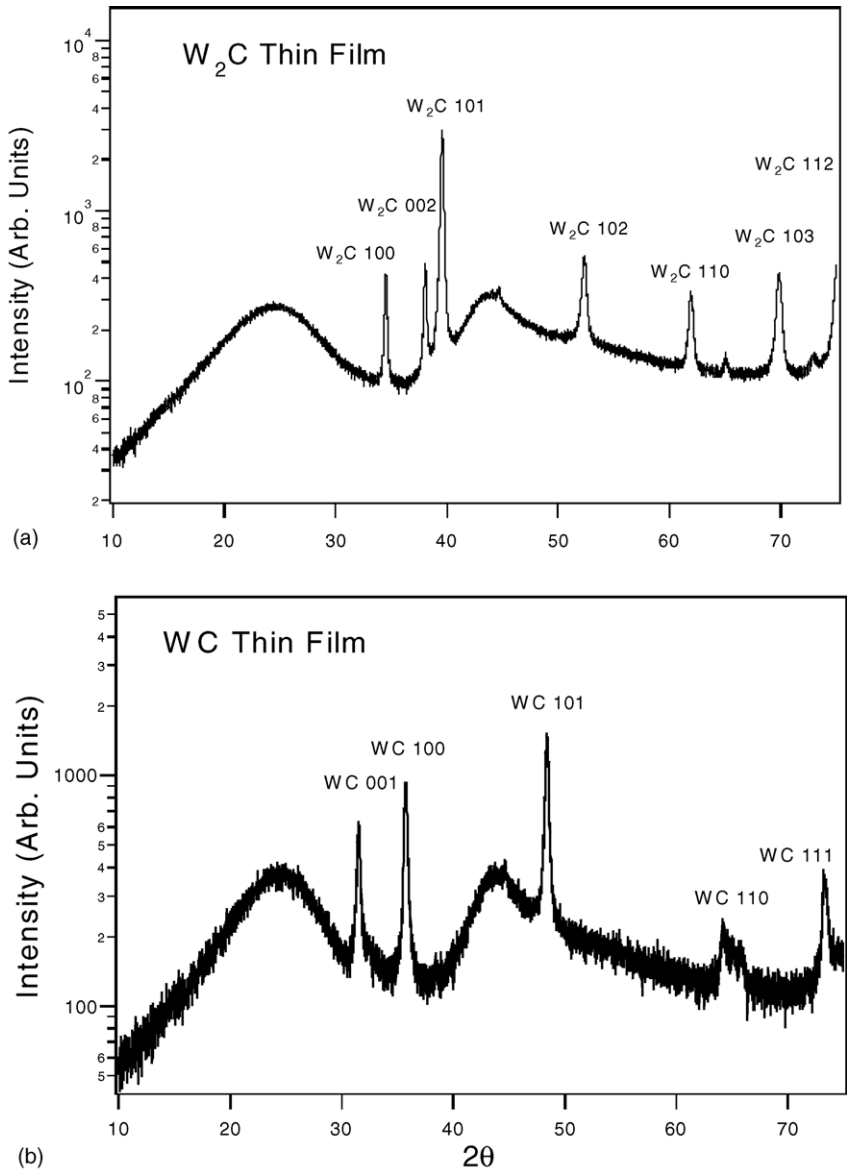

Fig. 1. XRD spectra of (a) phase pure W_2C and (b) phase pure WC thin films deposited on glassy carbon substrates.

sample was observed in the oxidation peak centered at ~0.92 V. Unlike W_2C, however, oxidation into W_xO_y species will not occur if the potential is held in the stable region below ~0.6 V, allowing WC to be potentially used as an electrocatalyst.

3.2.2. XPS measurements of electrochemical stability

Fig. 3 displays XPS results of WC and W_2C tungsten 4f peaks before and after electrochemical measurements in 0.5 M H_2SO_4. For comparison, the W 4f peak of a carbide-modified W(1 1 0) surface with atomic C/W = ~0.9 is also included. Prior to electrochemical measurements, the WC film exhibits W $4f_{5/2}$ and W $4f_{7/2}$ peaks at binding energies of 33.3 and 31.4 eV, respectively, which are very similar to those of the C/W(1 1 0) surface. After the CV measurement between −0.2 and 1.0 V and back to −0.2 V in a 0.5 M H_2SO_4 solution saturated with nitrogen, no significant spectroscopic changes were noticed. The observation suggests that the degree of WC oxidation is relatively minor during the CV measurement.

The W 4f XPS spectrum of W_2C before electrochemical measurements revealed four distinct features: carbide-modified W at 33.7 and 31.4 eV, and oxygen-modified W at 37.3 and 35.4 eV. The detection of oxygen-modified peaks was due to the oxidation of the W_2C film by air while being transferred from the PVD deposition chamber to the UHV XPS chamber. After performing electrochemical CV measurements, the W 4f peaks were completely converted to those of oxygen-modified W. The XPS results indicated that the surface regions of W_2C, within the detection limit of

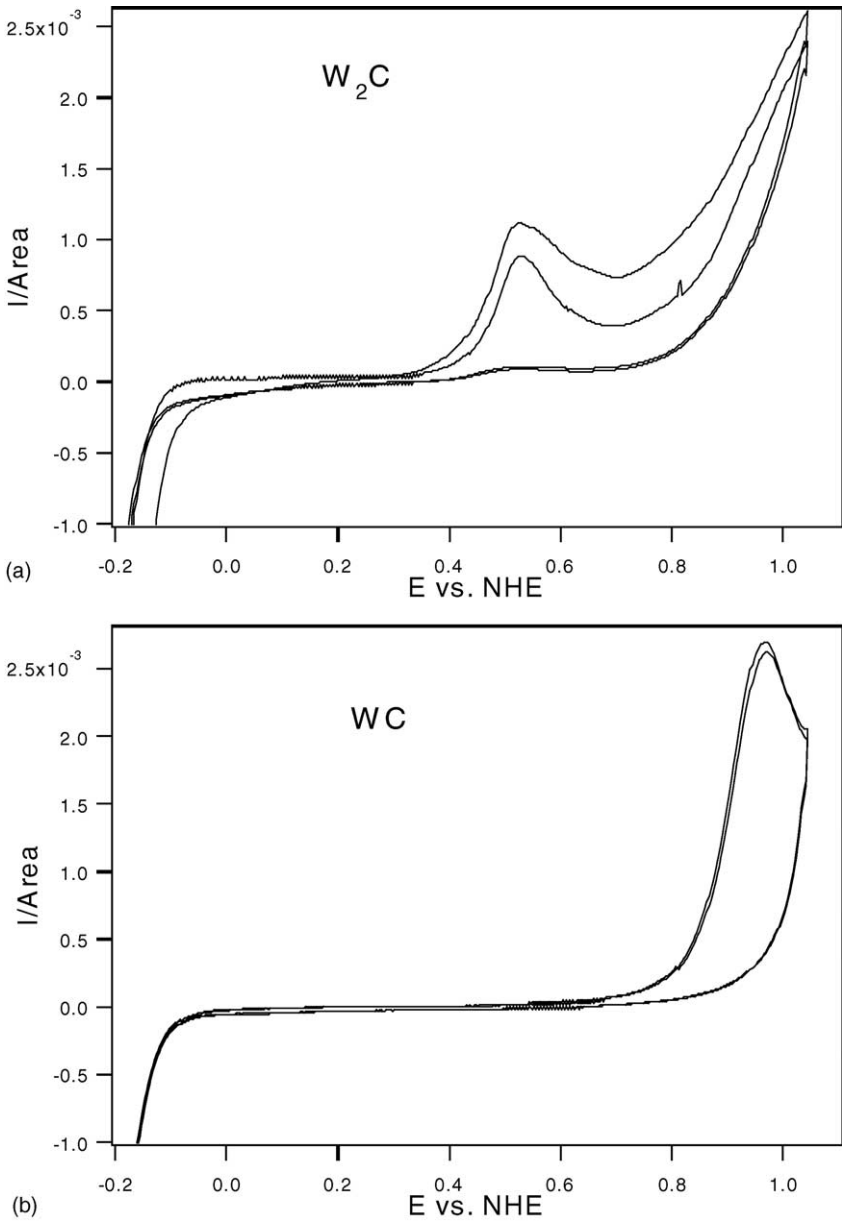

Fig. 2. Electrochemical CV measurements performed in 0.5 M H_2SO_4 saturated with N_2 of (a) W_2C and (b) WC films on carbon paper. For measurements, a 45 s conditioning period holding the working electrode at 0.05 V and a linear ramping rate of 10 mV/s were used was used from −0.2 to 1.0 V and then back to −0.2 V. The CV curves were measured following two consecutive cycles. Voltages are normalized with respect to the normal hydrogen electrode.

XPS, were completely oxidized during the CV measurements.

3.3. Surface science studies of methanol on WC and Pt/WC films

Surface science studies were performed on the relatively stable WC film. The objectives of these studies were primarily two-fold: (1) to determine whether the WC film was active toward the dissociation of methanol, and (2) to determine whether the presence of low coverages of Pt would promote the surface activity of the WC film.

HREEL spectra following the decomposition of adsorbed CH_3OH on clean and Pt-modified WC thin films are described in this section. The exposures of methanol were made with the film temperature at <150 K; the adsorbed layer was then heated to the indicated temperatures, held at the temperature for 1 min, and cooled before the HREEL spectra were recorded. Finally, the height of the elastic peaks in all spectra have been normalized to unity, and the expansion factor for each individual spectrum represents the multiplication factor relative to the elastic peak.

HREEL spectra monitoring the thermal decomposition of 40 L CH_3OH and 30 L CD_3OH adsorbed on a clean WC film

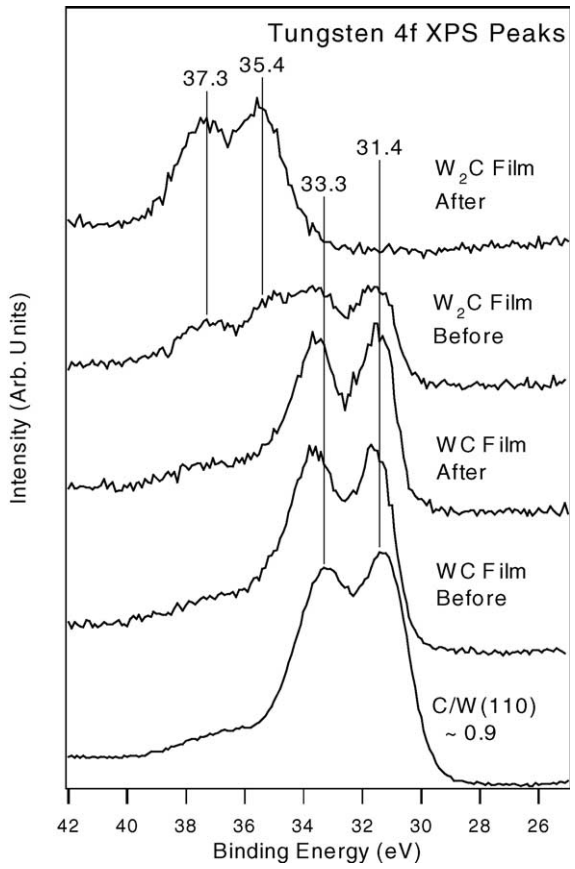

Fig. 3. W 4f WC and W_2C XPS spectra, before and after electrochemical measurements. W 4f XPS spectra of carbide-modified W(1 1 0) with C/W ~0.9 is also included.

are shown in Fig. 4. At 200 K, the vibrational modes of these layers are observed as follows (the frequencies for CD_3OH are in parentheses): 1028 (1021) cm^{-1}, ν(CO); 1157 (900) cm^{-1}, $\gamma(CH_3)$; 1461 cm^{-1}, $\delta(CH_3)$; 2848 (2070) cm^{-1}, $\nu_s(CH_3)$; and 2989 (2232) cm^{-1}, $\nu_{as}(CH_3)$. A weak CO peak due to the adsorption of CO from the UHV background, is detected at 2029 cm^{-1}.

Although a weak ν(OH) feature at ~3599 cm^{-1} is present due to accumulation of background H_2O, it is important to note the lack of the characteristic ν(OH) feature of molecular methanol at ~3240 cm^{-1}. The absence of this feature indicates the scission of the methanol O–H bond on the WC film at 200 K. The vibrational assignments of the resulting methoxy (CH_3O, CD_3O) species on WC thin films are compared to methoxy on C/W(1 1 1) [1] and C/W(1 1 0) [4] in Table 1. When the layers are heated to 400 K, the following changes are observed: (1) a decrease in the intensities related to the CH_3 (and CD_3) modes; (2) a decrease in the intensity of the ν(CO) mode at 1028 (1021) cm^{-1}; and (3) the growth of a ν(W–O) mode at 521 (500) cm^{-1}. Further heating to 500 K produces no significant spectroscopic changes, indicating that the methoxy intermediate is stable between 400 and 500 K.

Fig. 5 shows the HREEL spectra following the thermal decomposition of 40 L CH_3OH adsorbed on a 0.8 ML (monolayer) Pt-modified WC film. The HREEL spectrum at 200 K shows the following features: 419 cm^{-1}, ν(metal–O); 1028 cm^{-1}, ν(CO); 1170 cm^{-1}, $\gamma(CH_3)$; 1468 cm^{-1}, $\delta(CH_3)$; and 3004 cm^{-1}, $\nu_{as}(CH_3)$; as well as a CO peak from background adsorption at 2070 cm^{-1}. Similar to that observed on clean WC, the scission of the O–H bond to produce methoxy also occurs on 0.8 ML Pt/WC film at 200 K, as indicated by the absence of a ν(OH) feature at ~3240 cm^{-1}. When the layers are heated to 400 K, the following spectroscopic changes occur: (1) a reduction of the intensities of peaks related to CH_3 vibrational modes; (2) a reduction of intensity of the ν(CO) vibrational mode at 1028 cm^{-1}; (3) the growth of the ν(metal–O) or ν(metal–C) feature at 419 cm^{-1}. Further heating the layers to 500 K results in a continued reduction of the intensities of peaks related to the vibrational modes of methoxy. This observation is different from that on the clean WC film, which does not show further decomposition of methoxy at temperatures between 400 and 500 K. Such comparison suggests that the presence of submonolayer Pt promotes the dissociation of methoxy, which is consistent with our previous studies of the dissociation of methoxy on Pt-modified C/W(1 1 1) [2]. As described in our previous studies on Pt/C/W(1 1 1) using HREELS and temperature programmed desorption (TPD) [2], the subsequent dissociation of the methoxy species leads to the production of atomic hydrogen and carbon on the surface. More detailed HREELS and TPD studies are needed to determine the decomposition mechanisms of methoxy on the Pt/WC PVD films.

3.4. Adsorption of H_2O and CO on WC and Pt-modified WC films

The adsorption and reaction of H_2O and CO are also important steps in the anodic chemistry of DMFC. We have

Table 1
Vibrational frequencies (cm^{-1}) of methoxy (CH_3O and CD_3O) on C/W(1 1 1), C/W(1 1 0), and WC thin film

Mode	$CH_3O(CD_3O)$/C/W(1 1 1)	ν_H/ν_D	$CH_3O(CD_3O)$/C/W(1 1 0)	ν_H/ν_D	$CH_3O(CD_3O)$/WC	ν_H/ν_D
ν(Metal–O)	534 (487)	1.10	561 (561)	1.00	(500)	
ν(CO)	1021 (974)	1.05	994 (981)	1.01	1028 (1021)	1.01
$\gamma(CH_3)$	1157 (906)	1.28	1157 (900)	1.29	1157 (900)	1.29
$\delta(CH_3)$	1448 (1069)	1.35	1448 (1069)	1.35	1461	
$\nu_s(CH_3)$	(2063)		(2056)		2848 (2070)	1.37
$\nu_{as}(CH_3)$	2956 (2226)	1.33	2943 (2212)	1.33	2989 (2232)	1.34

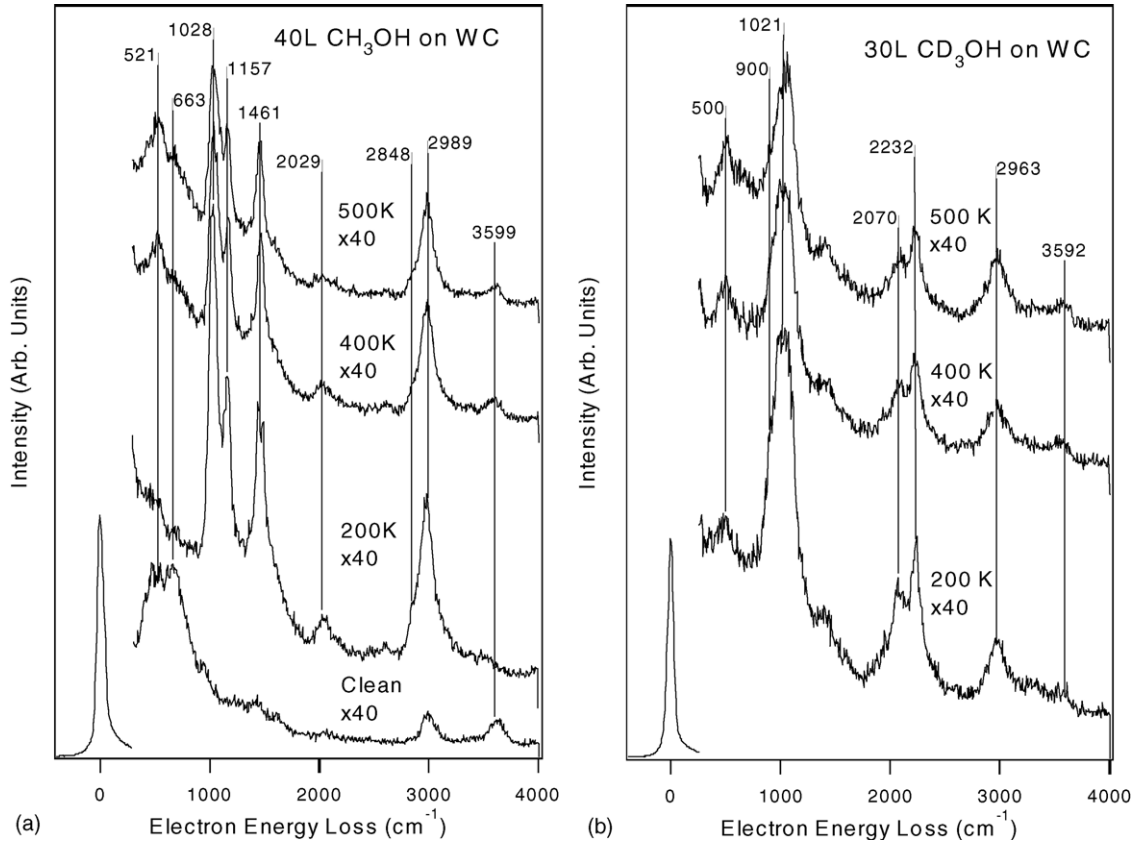

Fig. 4. HREEL spectra monitoring the thermal decomposition of (a) 40 L CH_3OH and (b) 30 L CD_3OH on the WC film.

performed preliminary HREELS studies following the adsorption of these two molecules on WC and Pt-modified WC surfaces. Fig. 6 shows HREEL spectra of 40 L H_2O on WC and 0.8 ML Pt/WC at 200 K. The detection of the characteristic δ(HOH) mode at 1624 cm^{-1} confirms that molecular H_2O is present on both surfaces at 200 K. In addition, the ν(OH) mode at 3612 cm^{-1} can be assigned to either surface hydroxyl group, or to isolated (not hydrogen-bonded) H_2O. Similar to those observed in Fig. 5, the ~2989 cm^{-1} mode is related to the presence of hydrocarbon fragments from the ''clean'' WC surface.

Fig. 7 shows the HREEL spectra following the exposure of 40 L CO to WC and 0.8 ML Pt/WC at 200 K. On both surfaces, the ν(metal–CO) and ν(CO) modes are observed at 399 and 2097 cm^{-1}, respectively. The ν(CO) mode is sharper and more intense on the 0.8 ML Pt/WC surface.

The results in Figs. 6 and 7 indicate that both H_2O and CO adsorbed molecularly on WC and 0.8 ML Pt/WC at 200 K. We did not perform detailed HREELS studies of the thermally induced dissociation or desorption due to the complexity caused by the re-adsorption of these two molecules during HREELS acquisition. More detailed studies will be performed using temperature programmed desorption (TPD) to follow the desorption and reaction of CO and H_2O on WC and Pt/WC.

4. Discussion

4.1. Stability of WC and W_2C in electrochemical environment

The XRD measurements confirm that phase pure WC and W_2C thin films are produced via magnetron sputtering (Fig. 1). The XPS results of the two surfaces (Fig. 3), after exposure to air during sample transfer, reveal that W_2C begins to oxidize immediately at atmospheric conditions, while WC is relatively stable. This is evident by the appearance of oxygen-modified W $4f_{5/2}$ and W $4f_{7/2}$ in the W_2C XPS spectrum and the absence of these features in WC. The different stability of W_2C and WC is also confirmed in the electrochemical CV measurements in 0.5 M H_2SO_4 saturated with N_2 (Fig. 2). WC remains stable for potentials between −0.1 and ~0.6 V, as evident by a lack of oxidation current in the CV curve. At potentials greater than 0.6 V, the potentiostat begins recording current due to oxidation of the WC film. The formation of W_xO_y species is detrimental to the electrocatalytic properties of the sample, blocking the active sites for fuel oxidation. However, if the anode potential is kept at less than 0.6 V, WC will act as an electrocatalyst without being oxidized. In contrast, the W_2C film does not have a stable region and begins to oxidize into W_xO_y species at potentials as low as −0.1 V. This is also

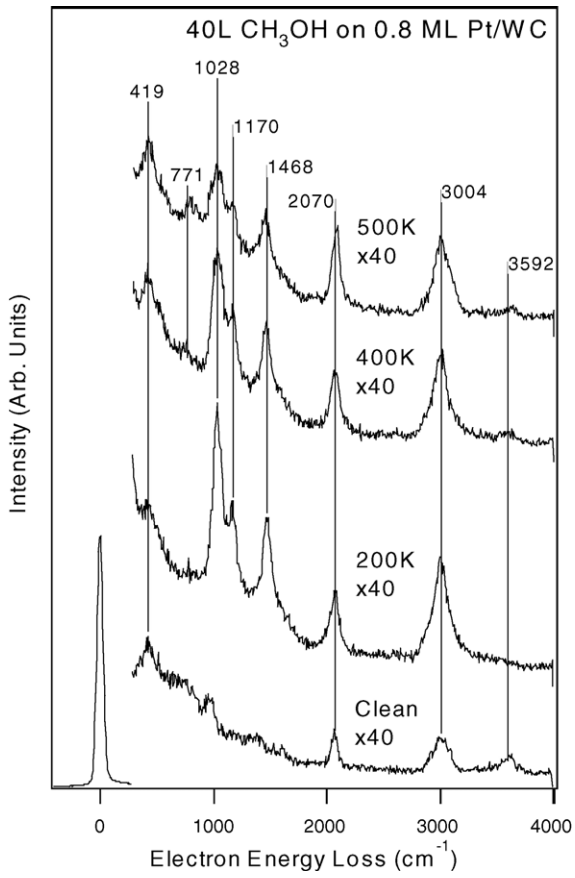

Fig. 5. HREEL spectra monitoring the thermal decomposition of 40 L CH_3OH on (a) 0.8 ML Pt-modified WC film.

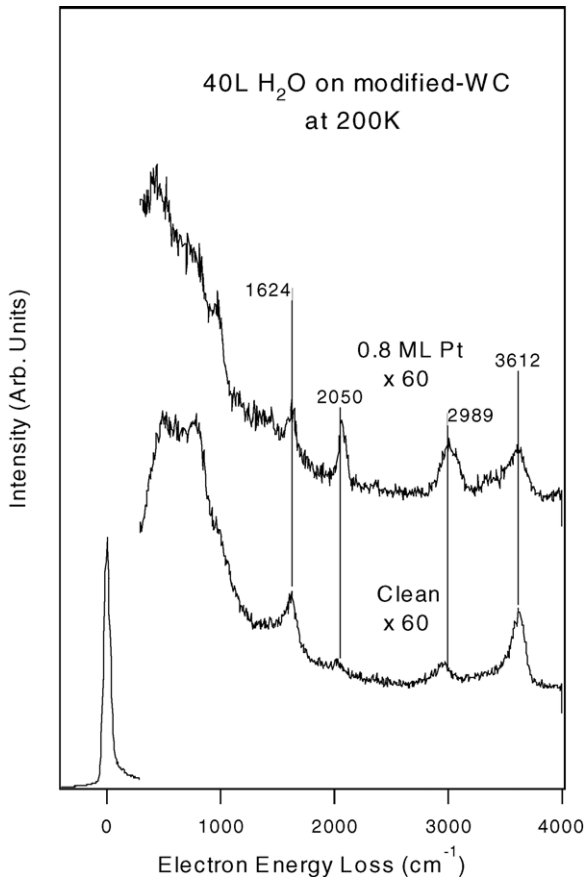

Fig. 6. HREEL spectra monitoring the adsorption of 40 L H_2O on clean WC film, 0.8 ML Pt-modified WC thin film at 200 K.

apparent by the decrease in anodic current during multiple CV cycles of W_2C in 0.5 M H_2SO_4 saturated with N_2. The oxidation of W_2C to W_xO_y species is also confirmed by XPS measurements (Fig. 3) after the CV measurements. The oxidation of W_2C occurs within the sampling depth of XPS (~30 Å), indicating that W_2C will not be an efficient electrocatalyst. In contrast, the degree of WC oxidation is relatively minor, as indicated by the near absence of oxidized W even after multiple cycles of CV measurements between −0.2 and 1.0 V.

4.2. Surface science studies of WC and 0.8 ML Pt/WC films

On clean WC and 0.8 ML Pt/WC films, adsorption of methanol results in the cleavage of the O–H bond to form methoxy at 200 K. This is evident by absence of a ν(OH) feature at ~3240 cm^{-1} (Figs. 4 and 5). The most interesting difference between the two surfaces is the stability of methoxy at temperatures between 400 and 500 K. On WC the methoxy species appear to be stable in this temperature range, as indicated by the very similar HREEL spectra at 400 and 500 K. In contrast, the presence of 0.8 ML Pt causes a significant reduction of the intensities of the methoxy vibrational modes. This observation suggests that submonolayer coverages of Pt promote the dissociation of methoxy. It is important to point out that, under UHV conditions, bulk Pt single crystal surfaces such as Pt(1 1 1) are nearly inert toward the complete dissociation of methanol [24]. Therefore, the reactivity observed on the 0.8 ML Pt/WC surface suggests the possibility of a synergistic effect by supporting submonolayer Pt on WC, which is consistent with our earlier studies of the dissociation of methanol on Pt-modified C/W(1 1 1) [2].

In addition, the adsorption of H_2O on the electrocatalyst is critical in the oxidation and removal of the CO reaction intermediate from the decomposition of methanol [6–8]. HREELS results (Fig. 6) indicate that both WC and 0.8 ML Pt/WC surfaces adsorb molecular water at 200 K. It is useful to point out that, under UHV conditions, H_2O does not adsorb on bulk Pt single crystals such as Pt(1 1 1) at 200 K [24].

Overall, the surface science results indicate that the WC and 0.8 ML Pt/WC surfaces show favorable properties as compared to bulk Pt single crystals. The WC and Pt/WC surfaces are more active toward the dissociation of methanol and toward the adsorption of molecular water at 200 K more detailed studies of the reaction mechanisms and desorption temperatures of methanol, water, and CO are underway using TPD.

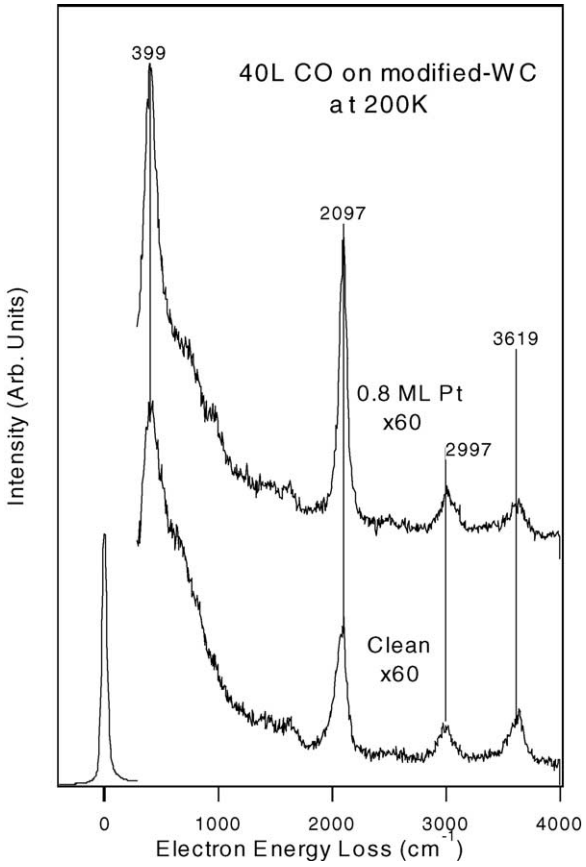

Fig. 7. HREEL spectra following the adsorption of CO on WC and 0.8 ML Pt/WC at 200 K.

Finally, the surface science results demonstrate the promoting effect of submonolayer Pt for the dissociation of methanol on WC. Such observation suggests the possibility of promoting WC electrocatalysts with low coverages of Pt for DMFC. The synthesis of WC and Pt/WC, as well as electrooxidation of methanol over these films, are currently underway.

5. Conclusions

From the results and discussion presented above, the following conclusions can be made regarding the surface science and electrochemical studies of W_2C, WC, and Pt/WC films:

(1) The combination of electrochemical CV measurements and XPS show that the WC film is stable at anode potentials below 0.6 V, demonstrating the potential use of WC as an anodic electrocatalyst in the DMFC. In contrast, W_2C does not have a stable region, causing immediate oxidation to form W_xO_y species when exposed to air or in an electrochemical environment.
(2) On clean WC, methanol adsorbs as methoxy via cleavage of the O–H bond in methanol at 200 K. The methoxy intermediate is stable to 500 K.
(3) On 0.8 ML Pt-modified WC film, methanol adsorbs as methoxy via cleavage of the O–H bond at 200 K. However, the presence of Pt promotes the further decomposition of methoxy between 400 and 500 K.
(4) Water and CO adsorb molecularly on clean WC and 0.8 ML Pt/WC at 200 K, providing the possibility for future studies of the reaction between H_2O and CO at higher temperatures.
(5) Additional surface science and electrochemical studies are underway to determine the feasibility of using WC and Pt/WC for the electrooxidation of methanol.

Acknowledgments

We acknowledge financial support from Basic Energy Sciences of the Department of Energy (DOE/BES Grant no. DE-FG02-04ER15501). We also acknowledge contributions at the initial phase of the project from Dr. Henry Hwu, Lijie Bao and Dr. Kourtakis. MBZ acknowledges partial financial support from a National Aeronautics and Space Administration Fellowship Grant #NGT5-40024, the University of Delaware Dean's Fellowship, and the Bill Barron Fellowship.

References

[1] H.H. Hwu, J.G. Chen, K. Kourtakis, J. Gerry Lavin, J. Phys. Chem. B 105 (2001) 10037.
[2] N. Liu, K. Kourtakis, J.C. Figueroa, J.G. Chen, J. Catal. 215 (2003) 254.
[3] H.H. Hwu, B.D. Polizzotti, J.G. Chen, J. Phys. Chem. B 105 (2001) 10045.
[4] H.H. Hwu, J.G. Chen, J. Phys. Chem. B 107 (2003) 2029.
[5] A. Hamnett, Catal. Today 38 (1997) 445.
[6] R. Parsons, T. VanderNoot, J. Electroanal. Chem. 257 (1998) 9.
[7] A. Hamnett, B.J. Kennedy, Electrochim. Acta 33 (1988) 1613.
[8] M.M.P. Janssen, J. Moolhuysen, Electrochim. Acta 21 (1976) 869.
[9] J.G. Chen, M.D. Weisel, Z.-M. Liu, J.M. White, J. Am. Chem. Soc. 115 (1993) 8875.
[10] B. Fruhberger, J.G. Chen, J. Am. Chem. Soc. 118 (1996) 11599.
[11] J. Eng Jr., B.E. Bent, B. Fruhberger, J.G. Chen, Langmuir 14 (1998) 1301.
[12] N. Liu, S.A. Rykov, H.H. Hwu, M.T. Buelow, J.G. Chen, J. Phys. Chem. B 105 (2001) 3894.
[13] B.D. Polizzotti, H.H. Hwu, J.G. Chen, Surf. Sci. 520 (2002) 97.
[14] H.H. Hwu, J.G. Chen, Surf. Sci. 557 (2004) 144.
[15] R. Levy, M. Boudart, Science 181 (1973) 547.
[16] H. Boehm, F.A. Pohl, Wiss. Ber. AEG-Telefunken 41 (1968) 46.
[17] H. Binder, A. Koehling, G. Sandstede, Am. Chem. Soc. Div. Fuel Chem. Prepr. 13 (1969) 99.
[18] Zellner, Hwu, Chen, Surf. Sci. 56 (2004) 89.
[19] M.B. Zellner, R.W. Birkmire, E. Eser, W.N. Shafarman, J.G. Chen, Prog. Photovolt:Res. Appl. 11 (2003) 543.
[20] Neetha, Zellner, Chen, Surf. Sci. 556 (2004) 87.
[21] C. Liang, F. Tian, Z. Wei, Q. Xin, C. Li, Nanotechnology 14 (2003) 955.
[22] R.S. Lima, J. Karthikeyan, C.M. Kay, J. Lindemann, C.C. Berndt, Thin Solid Films 416 (2002) 129.
[23] P. Colpo, T. Meziani, P. Sauvageot, G. Ceccone, P.N. Gibson, F. Rossi, J. Vac. Sci. Technol. A 20 (5) (2002) 1632.
[24] S.K. Jo, J. Kiss, J.A. Polanco, J.M. White, Surf. Sci. 253 (1991) 233.